NOAA Technical Memorandum ERL PMEL-60

CURRENT INVENTORY OF ANTHROPOGENIC CARBON DIOXIDE IN THE NORTH PACIFIC SUBARCTIC GYRE

J. D. Cline
R. A. Feely
K. Kelly-Hansen
J. F. Gendron
D. P. Wisegarver
C. T. Chen

Pacific Marine Environmental Laboratory
Seattle, Washington
March 1985

UNITED STATES
DEPARTMENT OF COMMERCE

Malcolm Baldrige,
Secretary

NATIONAL OCEANIC AND
ATMOSPHERIC ADMINISTRATION

Environmental Research
Laboratories

Vernon E. Derr,
Director

NOTICE

Mention of a commercial company or product does not constitute an endorsement by NOAA Environmental Research Laboratories. Use for publicity or advertising purposes of information from this publication concerning proprietary products or the tests of such products is not authorized.

TABLE OF CONTENTS

	Page
1.0 Summary	1
2.0 Introduction	3
3.0 Methods	5
3.1 Analysis of F-11	5
3.2 Analysis for Total Carbon Dioxide, Total Alkalinity and Nutrients	7
4.0 Models	8
4.1 Vertical Diffusion-Advection Model	8
4.2 Vertical Mixing Parameters Derived from the Distribution of F-11	13
4.3 CO_2 Source Function	17
4.4 Back-Calculation Method for Excess CO_2	19
4.5 Excess TCO_2 Model and Source Function	23
5.0 Results and Discussion	25
5.1 Excess CO_2 Model Predictions	25
5.2 Model Predictions of Excess CO_2 in the North Pacific Gyre	28
6.0 Conclusions	29
References	31
Appendix 1	37

1.0 SUMMARY

The most significant environmental issue of the next century will be systematic changes in the earth's climate due to increases in the atmospheric burden of carbon dioxide. This secular increase is the result of the burning of fossil fuels and massive deforestation currently underway. Since 1958, the atmospheric CO_2 concentration has risen from about 315 ppm to about 343 ppm; an average rate of 0.4%/yr. Current wisdom places the preindustrial atmosphere at 270 ± 10 ppm.

The major repositories for anthropogenic CO_2 are the oceans and the atmosphere. Of the total that has been released, approximately 50% resides in each of these reservoirs. Recent calculations suggest that the terrestrial biosphere has been a source, approximately equal in magnitude to the cummulative fossil fuel input during the past 150 years. Potentially the oceans represent a large reservoir for CO_2 because of the carbonate equilibria. However, only the surface layers are in equilibrium with the atmosphere, the remainder will be slow to come to equilibrium because most of the oceanic reservior is isolated from the atmosphere. The uptake of CO_2 by the oceans ultimately depends on the rate of vertical convection and mixing within the ocean thermocline, which in turn is coupled to large scale wind-driven and thermohaline circulation. Because the ocean thermocline is not stirred uniformly, we believe that the assimilation rate of CO_2 will be temporally and spatially variable. Thus, model predictions of the current CO_2 inventory as well as the uptake rate depend critically on the details of near-surface ocean circulation.

The distributions of freon-11, as a surogate tracer, have been combined with precise measurements of total carbon dioxide, total alkalinity, oxygen, nutrient and hydrography in order to estimate the amount of excess

CO_2 in the subarctic waters of the North Pacific gyre. The approach we employed utilizes the F-11 profiles to determine apparent vertical mixing parameters. These parameters were input into a horizontally averaged, one-dimensional vertical diffusion model along with a carbon dioxide source function to provide model predictions of anthropogenic (excess) CO_2 concentrations. These predictions were compared with observed estimates of excess CO_2, based on the back-calculation method using station data.

The results show very good agreement between the modeled profiles and the calculated data for all stations north of the subartic front. In the region of the front, the model assumptions are apparently not applicable due to the significance of lateral mixing. Our calculations indicate that approximately 4×10^{15} g of excess carbon, or about 2% of the total estimated fossil-fuel-derived carbon input now resides in the mixed layer and thermocline waters of the North Pacific gyre.

2.0 INTRODUCTION

The most significant environmental issue of the next century will be systematic changes in the earth's climate due to increases in the atmospheric burden of carbon dioxide (NRC, 1979; 1982). This secular increase is the result of the burning of fossil fuels and massive deforestation currently underway (Broecker and Peng, 1982). Since 1958, the atmospheric CO_2 concentration has risen from about 315 ppm to current levels of 343 ppm, or an average rate of 0.4%/yr. Present day estimates place the preindustrial atmosphere at between 260-280 ppm(v) (DOE, 1983).

The major repositories for anthropogenic CO_2 are the oceans and the atmosphere. Of the total that has been released, it is believed that approximately 50% resides in each of these reservoirs (Broecker *et al.*, 1979). Current wisdom suggests that the terrestrial biosphere was a significant source, approximately equal in magnitude to the fossil fuel input (Broecker and Peng, 1982), but the major contribution now is the burning of fossil fuels. Potentially the oceans represent a large reservoir for anthropogenic CO_2 because molecular CO_2 reacts with dissolved carbonate ions according to the reaction,

$$CO_2 + CO_3^{2-} + H_2O = 2HCO_3^- \ . \qquad (1)$$

However, only the immediate surface layers are in equilibrium with the atmosphere (Broecker *et al.*, 1979). The oceans as a whole will be slow to come to equilibrium because most of the oceanic reservior is isolated from the atmosphere (Bolin, 1960; Keeling, 1973; Broecker *et al.*, 1971). The uptake of CO_2 by the oceans ultimately depends on the rate of vertical convection and mixing within the ocean thermocline, which in turn is coupled to large scale wind-driven and thermohaline circulation (Sverdrup

et al., 1942). Because the ocean thermocline is not stirred uniformly, we believe that the assimilation rate of CO_2 will be temporally and spatially variable. Thus, model predictions of the current CO_2 inventory as well as the uptake rate will depend critically on the details of thermocline circulation.

The atmospheric concentration of CO_2 is a function of the rate of release of CO_2 to the atmosphere and its subsequent uptake by the oceans, assuming that the terrestrial biosphere is a source. Since the ocean, potentially, represents the largest repository for CO_2, the question becomes two-fold. The first is how much anthropogenic CO_2 is now in the oceans and secondly, where and at what rate is CO_2 being transported into the ocean? Because of complications in ocean circulation, the former may be easier to answer than the latter. In lieu of direct measurements of excess CO_2, the current inventory has been estimated separately from the distributions of various transient tracers (Oeschgar *et al.*, 1975; Broecker *et al.*, 1980). The tracers commonly applied to this problem are the traditional bomb transients (e.g., ^{3}H, ^{14}C), but ^{85}Kr and chlorofluoromethanes may also be appropriate (Broecker *et al.*, 1980; Gammon *et al.*, 1982). The usefulness of these various tracers lies in their known source functions and predictable behavior in the oceans. Using very simple models (e.g., box and continuous), these tracers are capable of defining one or two dimensional mixing characteristics that are needed to predict CO_2 coupling between the ocean and atmosphere (Bolin, 1960; Craig, 1957; Broecker *et al.*, 1971; Keeling, 1973; Oeschger *et al.*, 1975; and references contained therein). None of these models attempts to explain the physics of mixing, but is used diagnostically to predict CO_2 inventories and uptake rates based on parameterized transport coefficients.

It is important to note that none of the studies to date has attempted to correlate model predictions with excess CO_2 concentrations. The principal reason that this has not been done is the difficulty in reliably measuring the anthropogenic CO_2 signal in the oceans. However, some progress has been made in recent years on the precise measurement of total CO_2 and it is now possible to make estimates of excess CO_2 (Brewer, 1978; Chen and Millero, 1979).

In this report we summarize our investigations of the distribution of excess CO_2 in the subarctic gyre of the North Pacific. The approach we used is to estimate the concentration of excess CO_2 from precise measurements of total dissolved inorganic carbon, total alkalinity and nutrient concentrations, followed by the determination of apparent vertical mixing parameters from the distributions of F-11. This information is then combined iteratively to predict the excess CO_2 concentration in the main thermocline over the North Pacific (> 40°N).

3.0 METHODS

3.1 Analysis of F-11

Water samples were collected in rosette-mounted syringes (Cline *et al.*, 1982), fitted with Ni plated brass stopcocks and 13 ga. needles. The syringe was partially filled with seawater purged of freons to reduce the blank. Prior to lowering the rosette, the stopcocks were opened and the "zero" water forced from the sampler. On completion of the cast, the stopcocks were closed, needles removed, and samplers placed in a stainless steel tank filled with fresh seawater. The samples remained in the holding tank until analysis was complete, typically six hours.

The analytical system is similar to that described by Gammon *et al.* (1982). Dissolved gases were purged from 30 ml aliquots of the sample with purified nitrogen gas (Swinnerton and Linnenbom, 1967). The purged gases were dried by passage through K_2CO_3 and concentrated in a "U" trap (0.32 cm o.d. dia. stainless steel tubing) packed with Porasil C and maintained at -80°C. The trap was heated to approximately 85°C to release the freons for subsequent GC-EC analysis.

An initial separation of sample gases was accomplished with a short (~10 cm) precolumn of Porasil B (50°C). The primary function of this first precolumn was to partition the chlorofluoromethanes from the more slowly eluting compounds. This also permitted the quantitative retention of F-12 and N_2O on a 10 cm column of Molecular Sieve 5A (130°C) isolated by a four port valve, before F-11 had passed through the first precolumn. Once the F-11 had reached the detector, the column was opened to carrier flow and the separation of F-12 and N_2O was completed.

Final separation and detection of the freons were carried out on a Hewlett Packard 5730A gas chromatograph equipped with a constant current electron capture detector (15 μC ^{63}Ni) and a 3 m column of Porasil B. Detector response was quantified on a Hewlett Packard 3388A integrator. Standard gases and atmospheric samples were analyzed in the same manner.

The primary standard gas was calibrated by R. Rasmussen (Oregon Graduate Center) and Paul Goldan (NOAA Aeronomy Laboratory, Boulder). Cryo-pumped whole air samples were periodically collected at sea and used as secondary standards.

An examination of more than 100 duplicate analyses indicates a precision of ±0.02 pM/L for F-11 and F-12.

3.2 Analysis for Total Carbon Dioxide, Total Alkalinity and Nutrients

Total carbon dioxide (TCO_2) and total alkalinity (A_T) were determined from discrete water samples employing the potentiometric titration procedure described by Bos and Williams (1982). The method is based upon techniques developed by Gran (1952) and later modified by Dyrssen and Sillen (1967) and Edmond (1970). The titrations were performed with 0.25N Baker analytical grade HCl standardized against gravimetrically prepared sodium borate decahydrate solutions.

Water samples were collected in 30-L Niskin bottles and immediately transferred into 1-L glass stoppered bottles to which 1.0 mL of a saturated solution of $HgCl_2$ had been added to retard bacterial oxidation of organic matter prior to analysis. The samples were stored in a dark, cold-storage room at 4°C for as much as 12 hours. The samples were analyzed by the potentiometric method described above using a Brinkman E636 Titroprocessor linked to a Hewlett-Packard 85 computer. The data from the titroprocessor were automatically fed into the computer and processed using the modified Gran equations described in Bradshaw *et al.* (1981). Alkalinity contributions from boric, silicic and phosphoric acid were computed from equations similar to those presented by Takahasi *et al.* (1982) in the GEOSECS Pacific Expedition Report. Total borate concentration was computed using the relation of Culkin (1965). The first and second dissociation constants of carbonic acid and the first apparent dissociation constant of boric acid are from Almgren *et al.* (1977). Potassium chloride was used to adjust the ionic strength of the sodium tetraborate decahydrate standards to 0.7. At each station a blank was determined by titrating aliquots of a KCl solution containing no borate. The average blank was 4 μeq/L.

Figure 3.1 shows the station locations and Appendix 1 gives listings of the station number, depth, salinity, temperature, oxygen, nutrients, A_T and TCO_2 for the NOAA data from the western, central and eastern North Pacific cruises. For the eastern North Pacific TCO_2 and A_T data the analytical procedures are described fully in Chen (1982).

Samples for nitrate, phosphate and silicate were collected in 250 ml amber Nalgene bottles and immediately frozen for subsequent colorimetric analysis by the methods of Strickland and Parsons (1972) employing a Technicon Autoanalyzer.

4.0 MODELS

4.1 Vertical Diffusion-Advection Model

The distribution of a time dependent, non-conservative, chemical tracer is given by the equation (Sverdrup *et al.*, 1942),

$$C_t = K_H\{C_{xx} + C_{yy}\} + K_v C_{zz} - uC_x - vC_y - wC_z - R, \qquad (2)$$

where the subscripts indicate the first and second derivatives with respect to the space variables. The mean velocities in the x, y, z directions are u, v, and w; the horizontal and vertical eddy diffusivities are given by K_H and K_v. Any internal source or sink term is represented by R. Equation (2) is rarely solved in the above form because of insufficient temporal and spatial data, therefore simplifications are required.

The principal objective in the study is to predict the inventory of excess CO_2, using the simplest possible model. The first assumption is that the downward migration of CO_2 or freon-11 can be treated as a diapycnal process in the subarctic gyre. This is a reasonable assumption since deep

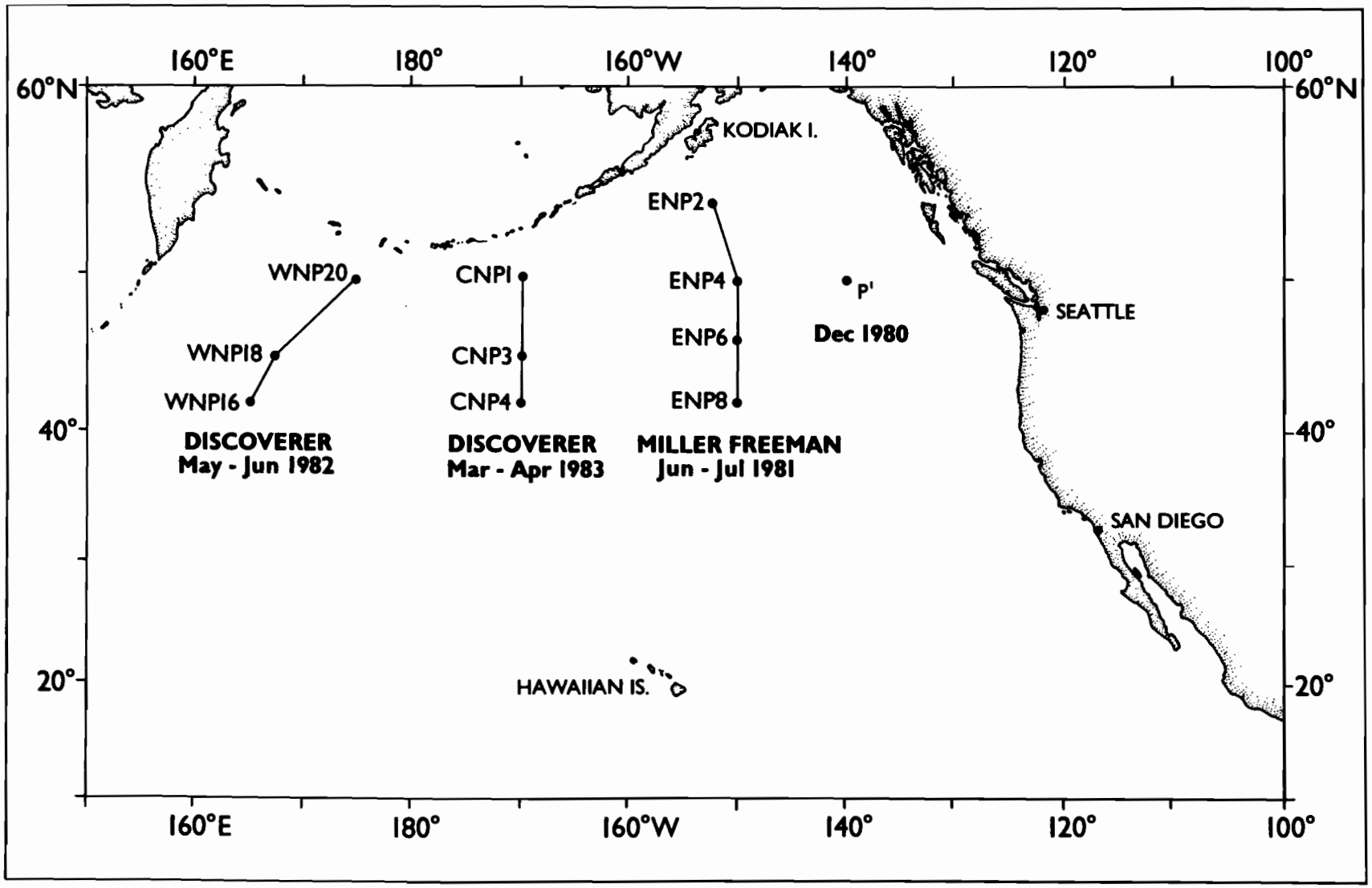

Figure 3.1 The location of stations occupied in the North Pacific Ocean. Stations shown in the North Pacific were sampled in May 1981, except P', which was sampled in December of 1980. Stations in the western North Pacific (WNP-) and central North Pacific (CNP-) were occupied in June 1982 and March 1983.

isopycnal outcropping is not prevalent anywhere in the North Pacific (Reid, 1973), nor is there deep convection. This is not to say that vertical diffusion is the most significant process, but rather that the net effect of all transport terms can be parameterized in terms of a simple, one-dimensional vertical diffusion model (Broecker and Peng, 1982). In reality, gaseous tracers such as freon-11 and CO_2 are probably responsive to winter mixing in the western North Pacific. Once injected below the seasonal thermocline, the tracers then can be recirculated in the subarctic cyclone (Cline *et al.*, 1984). There also may be lateral transport of freons at depth from the northern part of the subtropical gyre, but we cannot evaluate the significance of this process at the present time. The net result is that the one-dimensional model overwhelmingly simplifies the physics of mixing and transport, but retains its diagnostic value.

With the assumption that the horizontal terms are either zero or they uniquely cancel each other, and that freons are conservative, eqn. (2) reduces to

$$C_t = K_v C_{zz} - wC_z \tag{3}$$

where C is the concentration of F-11. The solution to equation (3) for constant K_v and w is

$$C(z,t) = \exp(-wz/2K_v) \int_0^t F(t') \, G(z,t-t')dt' \tag{4}$$

where $$G(z,t-t') = \frac{z}{2\sqrt{\pi K_v (t-t')^3}} \exp\{-z^2/4K_v(t-t') - w^2(t-t)/4K_v\}$$

The initial condition is that $C(0,t) = F(t')$ and boundary conditions are the $C(z,0) = 0$ and $C(\infty,t') = 0$. These initial and boundary conditions are appropriate, since F-11 has no known natural source in the ocean and its

history in the atmosphere is short compared to the ventilation time of the deep sea (Gammon *et al.*, 1982). To evaluate the integral given in (4) the source function for F-11 must be known.

Our best estimate of the historical growth of F-11 in the atmoshpere is that derived from industrial release data (McCarthy *et al.*, 1977) and the recent measurements of Khalil and Rasmussen (1981). By correcting the release rate for stratospheric loss, the industrial releases can be made to coincide with observations made subsequent to 1975 (Gammon *et al.*, 1982). These results are shown in Fig. 4.1 and are applicable to 45°N latitude in the eastern North Pacific.

The surface concentration of F-11 is directly proportional to its atmospheric partial pressure, $C' = \beta p$, where β is the Bunsen solubility coefficient and p is the atmospheric mixing ratio. The Bunsen coefficients, a function of salinity and temperature, were calculated from the measurements of Wisegarver and Cline (1984). Although the solubility dependence on salinity was not specifically determined, this error is estimated to be less that 3% for the range of salinities encountered in the North Pacific. The source function, $F(t')$, is the product of the atmospheric mixing ratio (Fig. 4.1) and the Bunsen coefficient. The Bunsen coefficient is largely a function of temperature, which was chosen at each station from the mean annual value at the base of the winter mixed layer (Robinson and Bauer, 1976; Levitus, 1982). In reality, gas exchange and vertical transport are enhanced winter by winter cooling and deep wind mixing, hence our choice of the mean annual temperature at the base of the winter mixed layer is an attempt to average a seasonal process.

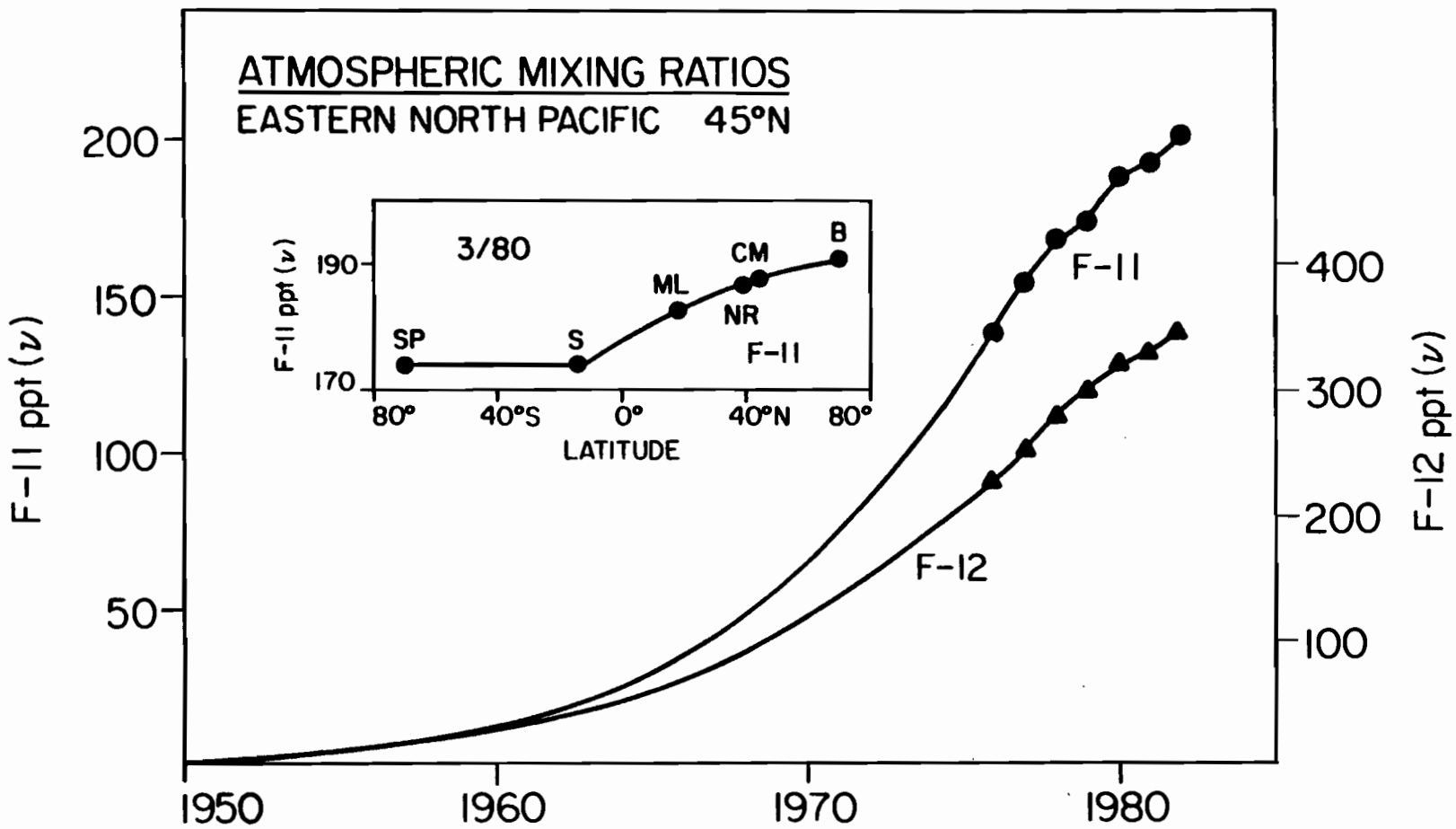

Figure 4.1 The temporal history of F-11 and F-12 in the atmosphere as constructed from industrial release data (Gammon *et al.*, 1982) and recent observations. Measured concentrations of F-11 (●) and F-12 (▲) at 45°N were made by Khalil and Rasmussen (1982).

4.2 Vertical Mixing Parameters Derived from the Distribution of F-11

The distribution of F-11 is used as a diagnostic scaler to determine the apparent vertical eddy diffusivity. This parameter is then used in conjunction with an estimate of the anthropogenic CO_2 source function to determine vertical profiles of excess CO_2. To demonstrate how this is accomplished, we will calculate K_v for station P′ located in the eastern North Pacific.

Station P′ was sampled repeatedly between 2-10 December 1980 for the distribution of F-11 and F-12. The model fit to these observations are shown in Fig. 4.2. The solid line indicates the best model fit (eqn. 4) to these data for $K_v = -9.4 \times 10^{+3} w + 0.35$ (cm^2/s), where w is the apparent vertical velocity ($w < 0$ upwelling). Unfortunately, the distribution of freon-11 is not particularily sensitive to specific values of K_v and w, but rather to their ratio or the scale height. The introduction of additional tracers not linearly dependent on F-11 might be useful in determining individual values of K_v and w, but clearly F-12 will not serve this purpose at P′ (see inset Fig. 4.2). However, our intention is not to detail the physics of mixing, but rather to predict the net effect of vertical transport. To accomplish this end we ignore the convective term (i.e., $w = 0$) and simply describe the vertical distribution of F-11 with the flux divergence, which at this station is 0.35 cm^2/s.

Using the simple one-dimensional model described above, we fit the observed distributions of F-11 at the stations shown in Fig. 3.1. The results of these calculations are shown in Table 4.1. In general, apparent vertical eddy diffusivities increase toward the south, with the smallest value (0.04 cm^2/s, Sta. WNP-20) found along the southern boundary of the Alaskan stream. This trend is expected from a one-dimensional model

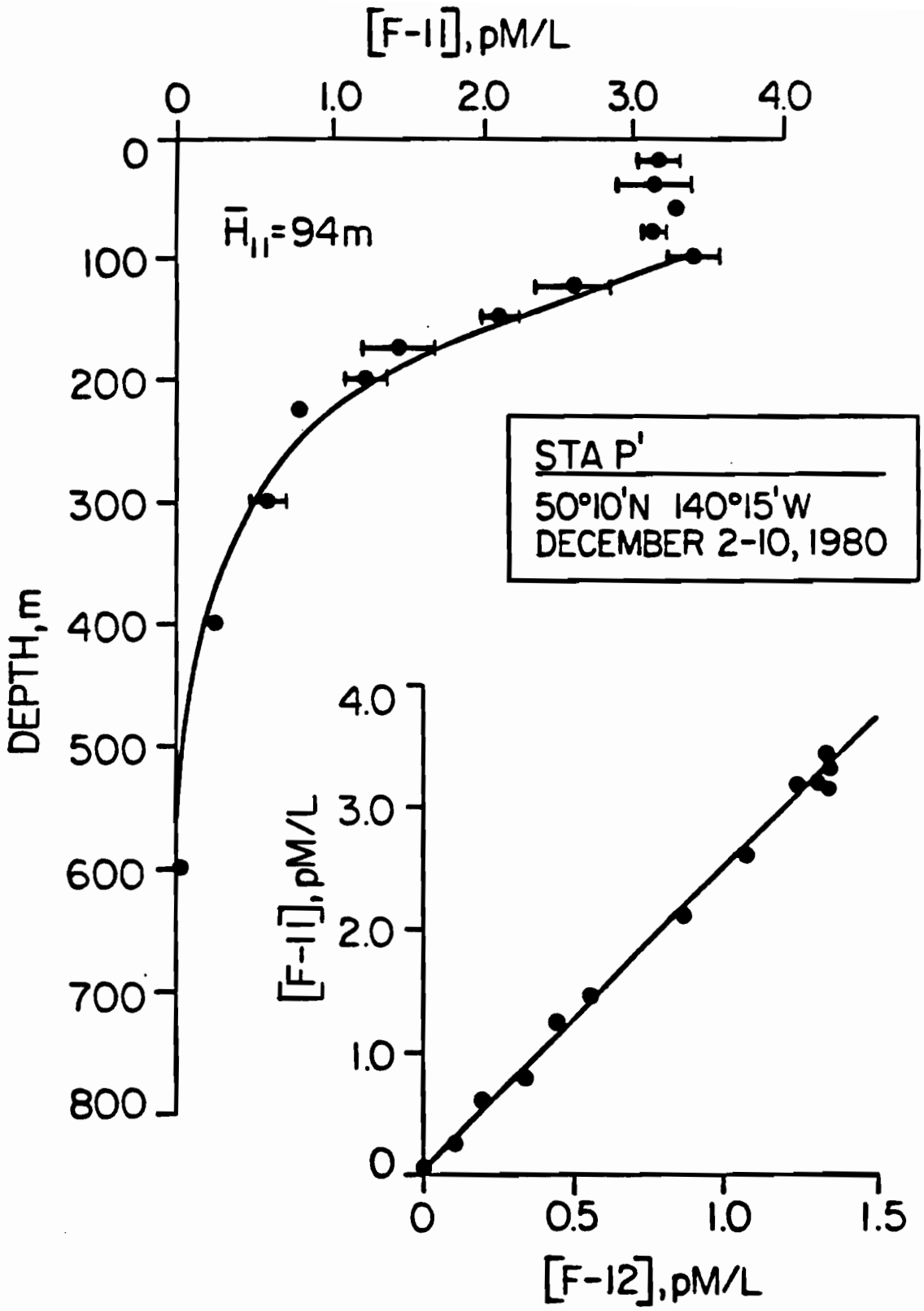

Figure 4.2 Freon-11 distribution at station P' in the North Pacific gyre. The inset shows a plot of freon-11 versus freon-12 concentrations at this station.

Table 4.1. Vertical mixing parameters in the North Pacific. The apparent vertical eddy diffusivity (K_v) and velocity (w) were obtained from a one-dimensional analysis of F-11. This tracer predicts the relationship $K_v = a \cdot w + K_v'$, where a is the scale height. Setting w = 0, the distribution is uniquely determined by the apparent vertical eddy diffusivity, K_v'.

Sta. No.	Lat	Long.	K_v	
	°N	°E/W	a·w	K_v'
		ENP		
NP-40	40°01'	134°57'W	$-9.7 \times 10^3 w$	0.70
NP-41	42°02'	129°55'W	---	0.28
P'	50°10'	140°15'W	$-9.4 \times 10^3 w$	0.35
		CNP		
CNP-1	50°00'	169°59'W	$-9.5 \times 10^3 w$	0.19
CNP-2	47°00'	169°59'W	$-1.2 \times 10^4 w$	0.33
CNP-4	42°00'	170°03'W	$-1.4 \times 10^4 w$	0.58
CNP-5	40°59'	170°01'W	$-2.7 \times 10^4 w$	1.9
CNP-6	40°01'	170°10'W	$-2.8 \times 10^4 w$	1.9
		WNP		
WNP-16	41°59'	165°03'E	---	---
WNP-18	45°19'	167°17'E	$-1.4 \times 10^4 w$	0.54
WNP-20	49°57'	175°00'E	$-4.8 \times 10^3 w$	0.04

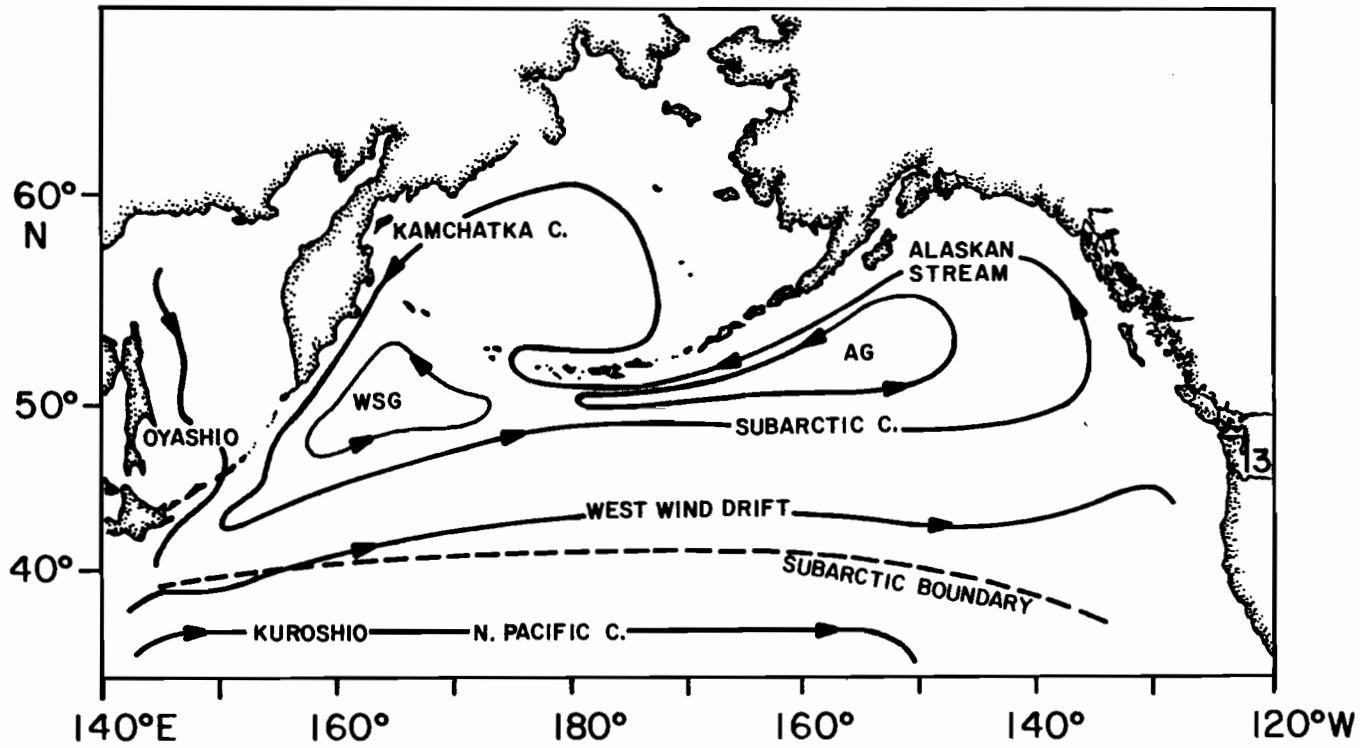

Figure 4.3 Streamlines showing major current systems in the North Pacific gyre (after Dodimead *et al.*, 1963).

because diapycnal processes are relatively more important within the subarctic gyre, whereas to the south near the subarctic front downwelling and isopycnal mixing become more significant (Roden, 1981). Because the latter processes are more energetic, K_v must be scaled upward to account for deeper penetration of the tracers. An apparent increase in K_v toward the south is expected, based on circulation and salt budget considerations within the North Pacific Gyre (Reid, 1965). There, the freshening of the surface layers from surface precipitation and runoff must be balanced by the vertical transport of salt if the salinity field is to remain stationary. Salt is also transported laterally into the upper thermocline from the subtropical gyre via the west wind drift and its northern extension, the Alaska stream (Fig. 4.3).

4.3 CO_2 Source Function

The uptake of CO_2 by the oceans is more complex than that of freons. This complexity arises because gaseous CO_2 reacts with water to form the aqueous species H_2CO_3, HCO_3^-, $CO_3^=$, and dissolved CO_2, or $(pCO_2)_{aq}$. The relative proportions of each are functions of the carbon dioxide and borate equilibria (Mehrbach *et al.*, 1973; Lyman, 1956; Millero, 1979; Almgren *et al.*, 1977). In practice, the concentration of each species can be estimated from measurements of total carbon dioxide (TCO_2) and alkalinity and, of course, the equilbrium constants (Bradshaw *et al.*, 1981). We are principally interested in the partial pressure difference in CO_2 (i.e., ΔpCO_2) across the air-sea interface, because it is this quantity that determines the flux.

Seasonally and spatially, the magnitude and direction of the flux of CO_2 is highly variable. This is due to local biological effects and to

surface warming and cooling, both of which influences the flux of gaseous CO_2. Thus, calculating a mean ocean flux of CO_2, even locally, would require a large data base. A more tractable approach is to assume that the ocean surface is near equilibrium with the atmosphere, so long as a suitable time average is taken. For our purposes here, that time need not be less than one year, since shorter term changes could not be tested observationally (see below). In essence then, if the atmospheric growth of CO_2 is known, then the partitioning of that CO_2 between the atmosphere and the ocean can be calculated from known thermodynamic quantities (Takahashi *et al.*, 1980).

Partitioning of CO_2 (equilibrium) between the ocean and the atmosphere is given in terms of the Revelle factor, R, where,

$$\frac{1}{R}\frac{d\{pCO_2\}}{\{pCO_2\}} = \frac{d\{TCO_2\}}{\{TCO_2\}}. \tag{5}$$

In this expression, TCO_2 is the sum of all carbon dioxide components. Although R is a function of temperature and the carbon dioxide components, we can assume that it has been relativley constant since pre-industrial times for water masses of constant temperature. Under these conditions, eqn (5) can be integrated over the interval of interest and yields the expression

$$\frac{\{pCO_2\}}{\{pCO_2\}_0}^{1/R} = \frac{\{TCO_2\}}{\{TCO_2\}_0}, \tag{6}$$

where the subscript '$_0$' reflects the initial boundary conditions, i.e., the value of pCO_2 and TCO_2 in 1825. However, what we are actually interested in is the change in fossil fuel CO_2 in the atmosphere since 1825, rather than the whole of the CO_2 signal. Changing to a Δ-notation requires that we substitute the following relationships into eqn (6)

$$\{\Delta pCO_2\} = \{pCO_2\} - \{pCO_2\}_0 \quad (7)$$

$$\{\Delta TCO_2\} = \{TCO_2\} - \{TCO_2\}_0. \quad (8)$$

We obtain after simplification and approximation the following:

$$\Delta TCO_2 = \frac{1}{R} \frac{\{TCO_2\}_0}{\{pCO_2\}_0} \Delta pCO_2 \quad (9)$$

This equation predicts a linear relationship between the incremental increase in atmospheric pCO_2 and dissolved TCO_2 in the ocean. As more and more CO_2 is added to the atmosphere, R increases and the ocean's ability to assimilate CO_2 is diminished. It should be emphasized that the relationship depicted in eqn. 9 holds only for a constant R.

Armed with the CO_2 source function and estimates of the vertical mixing parameters, we are now in a position to calculate ΔTCO_2 profiles for the North Pacific (>40°N) and compare them to observations derived from TCO_2 and total alkalinity measurements. First, however, we describe the method by which excess TCO_2 (ΔTCO_2) concentrations are determined.

4.4 Back-Calculation Method for Excess CO_2

Over the past few years several authors have employed a variety of different techniques to directly measure or estimate the oceanic CO_2 increase (Brewer, 1978; Chen and Millero, 1979; Chen and Pytkowicz, 1979; Takahashi *et al.*, 1983). The methods fall into two distinct categories. The first method involves direct measurements of CO_2 increases in surface waters from pCO_2 measurements made over time spans of several years to tens of years (i.e., Takahashi *et al.*, 1983). This method requires that accurate and precise pCO_2 measurements be made at the same location over

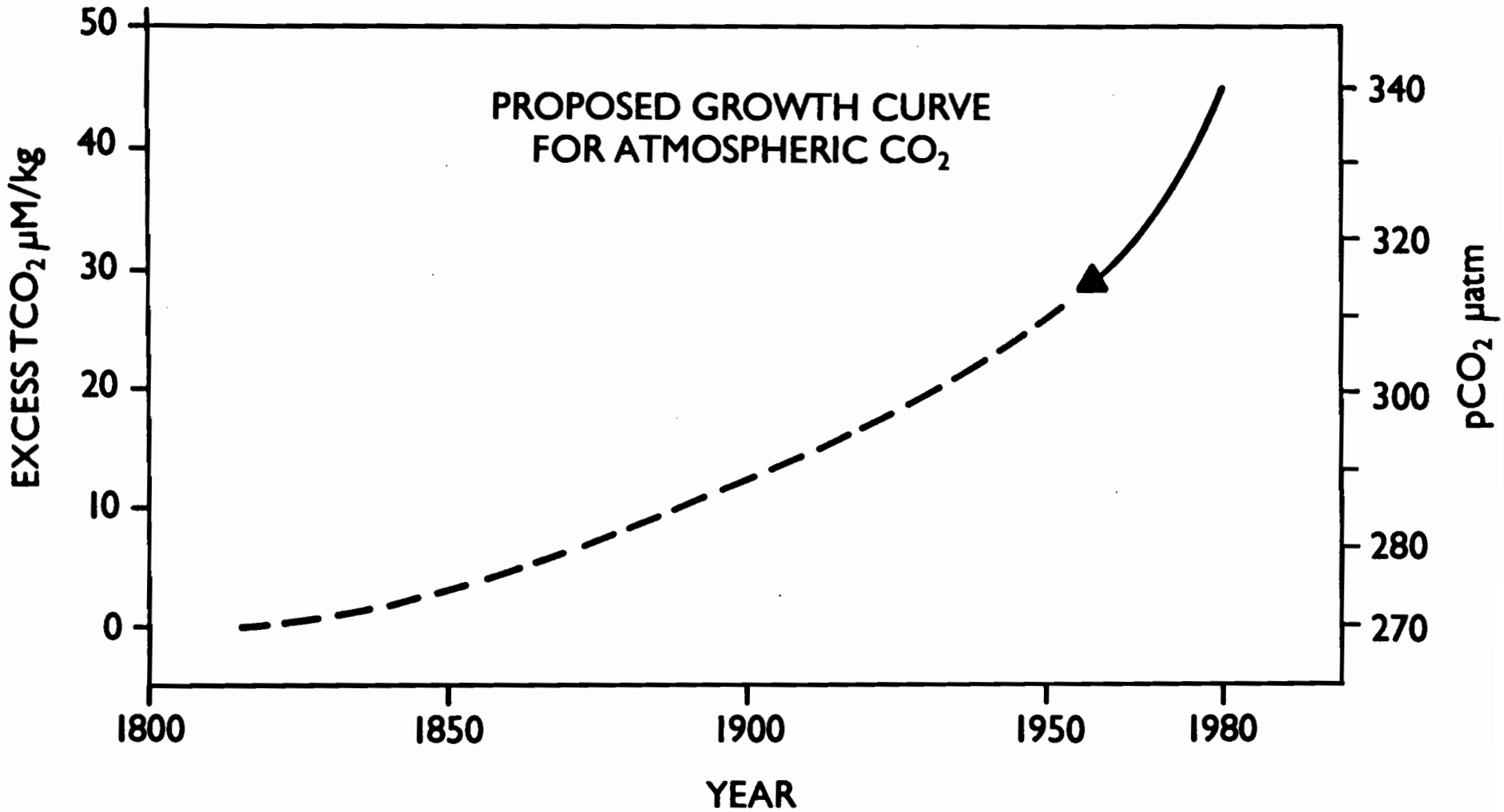

Figure 4.4 Excess CO_2 source function and atmospheric pCO_2 curve from 1820 to 1890. A pre-industrial value of 270 µatm was based on ice core data. The curve was fitted to include the atmospheric observations since 1958 (solid line).

long time intervals which, with the possible exception of the data for the North Atlantic, are not available in sufficient quantities to be useful for this purpose. The second less direct method involves a back-calculation of the CO_2 concentration of a parcel of water to its initial concentration at the sea surface after corrections have been made for changes due to biological decomposition of organic matter and dissolution of carbonate tests (i.e. Brewer, 1978). Specifically, the method assumes that a water parcel maintains a fixed degree of saturation with respect to atmospheric CO_2 at the sea surface. When the water parcel sinks, total CO_2 (TCO_2) is added by respiration and carbonate dissolution. The respiration-induced change in CO_2 can be calculated from the oxygen data employing the well-known Redfield ratios (Redfield *et al.*, 1963). The changes due to carbonate dissolution are calculated from the alkalinity changes. By correcting the data for these changes as well as for the preformed values of TCO_2 and total alkalinity, estimates can be made of the CO_2 concentration of the water parcel when it was last in contact with the atmosphere. These back-calculated CO_2 concentrations are then compared to obtain the oceanic CO_2 increase.

Both measurements suffer from relatively large uncertainties associated with the quality of the data and, in the case of the back-calculation method, natural deviations from the Redfield ratios (Shiller, 1981). However, it is possible to combine models of atmospheric input along with the direct measurement methods to make reasonable estimates of the fossil CO_2 inventory in the oceans.

The method for back-calculating the excess CO_2 signal is similar to the method reported by Chen (1982) and is summarized as follows:

$$\Delta TCO_2^\circ \ (\mu mol/kg) = TCO_2^\circ \ (present) - TCO_2^\circ \ (old)$$
$$= TCO_2^\circ \ (present) - [TCO_2 \ (measured) - 0.5 \ TA \ (measured)$$
$$- \alpha \ AOU + 0.5 \ TA^\circ \ (present)] \qquad (10)$$

where all quantities except AOU (Apparent Oxygen Utilization) are normalized to 35‰ S; ΔTCO_2° is a measure of the excess CO_2 signal; TCO_2° (old) and TCO_2° (present) are, respectively, the preformed total CO_2 values for a parcel of water formed sometime ago and for a water parcel formed at present; TCO_2 (measured) and TA (measured) are the measured concentrations of total CO_2 and titration alkalinity, respectively; TA° (present) is the present day preformed TA value; α is derived from the carbon-oxygen relationship for the data set presented in the manner prescribed by Chen and Pytkowitz (1979). The calculation of ΔTCO_2 using the equation above is subject to large uncertainties (Chen and Millero, 1979; Chen and Pytkowicz, 1979; Shiller, 1981; Chen *et al.*, 1982). The largest uncertainty is in the calculation of the TA° (present) and TCO_2° (present) values. The data from ENP, CNP, WNP (Appendix 1) indicate that TA° and TCO_2° can be represented by the following equations:

$$TA^\circ \ (\mu eg/kg) = 2361 - 1.2 \ \theta \ (\pm 10) \qquad \theta \leq 25^\circ C \qquad (11)$$

$$TCO_2^\circ \ (\mu mol/kg) = 2246 - 11 \ \theta \ (\pm 10) \qquad \theta \leq 24^\circ C \qquad (12)$$

where θ is the potential temperature and the numbers in parentheses give one standard deviation of the least-squares fit for the above equations. These equations are valid only for the North Pacific gyre.

4.5 Excess TCO_2 Model and Source Function

The one-dimensional model used to describe the vertical distribution of freon-11 is simplistic and is not intended to describe the actual mechanisms of vertical transport. At best, the model simply decribes the sum total of all processes leading to the vertical propagation of freon-11 in terms of an apparent eddy diffusivity (Broecker and Peng, 1982). This simple goal is, however, what we desire to accomplish, because our purpose here is to predict how much excess TCO_2 is in the North Pacific, not precisely how it got there. A much more elaborate model would be needed to accomplish that purpose.

The model we will use to predict the vertical distribution of excess TCO_2 is the same as that adopted for F-11, except the atmospheric source function is different. The assumption is that freons and ΔTCO_2 are conservative tracers, and that their respective source functions are spatially uniform between 40-55°N. This provides the freons with a unique characteristic because both bomb transients were not introduced into the North Pacific in a uniform way. This means that the source function for bomb-derived ^3H and ^{14}C are both space and time dependent, whereas those for freons and ΔTCO_2 are only time dependent, and better known.

To estimate the ΔTCO_2 profile for any specific location we need to have an estimate of the amount of anthropogenic CO_2 added since pre-industrial times as well as the rate at which it was added. The first of these can be derived from an estimate of the pre-industrial pCO_2 concentration and the Revelle factor, while the second is obtained by an iterative procedure until a match between the model curves and the observed ΔTCO_2 profiles are obtained. We begin by calculating the amount of excess TCO_2 present in the surface layers of the North Pacific subarctic gyre in 1980. This

quantity is independent of biological cycling, although to determine it analytically, one must account for seasonal changes in the TCO_2 pool.

We assume that the pre-industrial (1820) concentration of atmospheric CO_2 was 270 ppm. In 1980 it was 340 ppm, hence the change has been about 70 ppm. The fraction of this CO_2 that now resides in the ocean can be calculated from the equation (9) (Broecker *et al.*, 1971). Setting R = 11.5 ($5°C \leq T \leq 10°C$), ΔpCO_2 = 70 ppm, $[pCO_2]°$ = 270 ppm, and $[TCO_2]°$ = 2010 μm/kg (see below), the concentration of excess CO_2 in the North Pacific gyre is about 45 μm/kg. Having established theoretically and observationally the present day concentration of ΔTCO_2, we now only need to determine how pCO_2 has changed historically to calculate the inventory of excess CO_2 in the North Pacific gyre.

The time-dependent source function for pCO_2 is not known precisely and must be estimated from other tracer data. Broecker and Peng (1982) used a modified Oeschger model to determine the separate contributions from fossil fuel and forest and soil as a function of time. Their prediction results in a near-linear increase in pCO_2 since 1825 after combining the terrestrial and fossil fuel sources.

In this study we tested the pCO_2 curve postulated by Broecker and Peng (1982) by fitting model ΔTCO_2 profiles to the measured distributions. The source function we used is shown in Fig. 4.4 and is similar in shape to that proposed by Broecker and Peng. The only difference is the pre-industrial intercept, which we set to 270 ppm instead of 250 ppm. Raising the pre-industrial value to 270 ppm together with an assumed Revelle factor of 11.5 gives a better fit to the observed excess CO_2 concentrations in the mixed layer. However, uncertainties in observed

quantities as well as model assumptions do not permit us to be precise about the pre-industrial pCO_2 concentration.

5.0 RESULTS AND DISCUSSION

5.1 Excess CO_2 Model Predictions

Comparisons were made between the amount of excess CO_2 (ΔTCO_2) measured and the concentration predicted from the one-dimensional, time dependent diffusion model (see eqn. 3) at six stations in the subarctic gyre for the North Pacific. These are the only stations for which both excess CO_2 and freon observations were made simultaneously.

The results of the comparisons are shown in Fig. 5.1 for the ΔTCO_2 sources function given in Fig. 4.4. To make the correlation, we used the average mixed layer depth defined by the near-surface maximum in the observed ΔTCO_2, but relied on the model calculation (eqn. 9) to estimate the present day anomaly. As shown above, the calculated ΔTCO_2 concentration is about 45 μM/kg. The average of the observed mixed layer concentrations (see Fig. 5.1) is about 38 μM/kg, although the uncertainty is large. Photosynthesis and respiration in the mixed layer complicate an accurate measure of the present day surface ΔTCO_2^o concentration, hence we used the calculated value of 45 μM/kg as the mixed layer value.

Given that the concentration of excess CO_2 and the mixed layer depth appropriate to the total CO_2 concentration are not known precisely, the model fits to the observations shown in Fig. 4.1 are quite good. This is particularly surprising in view of the fact that the vertical eddy diffusivity varied from 0.04 cm^2/s to 1.2 cm^2/s. The profiles of ΔTCO_2, shown in Fig. 5.1, indicate a slight deepening of the profiles from north to south, which corresponds with the increase in apparent vertical mixing towards

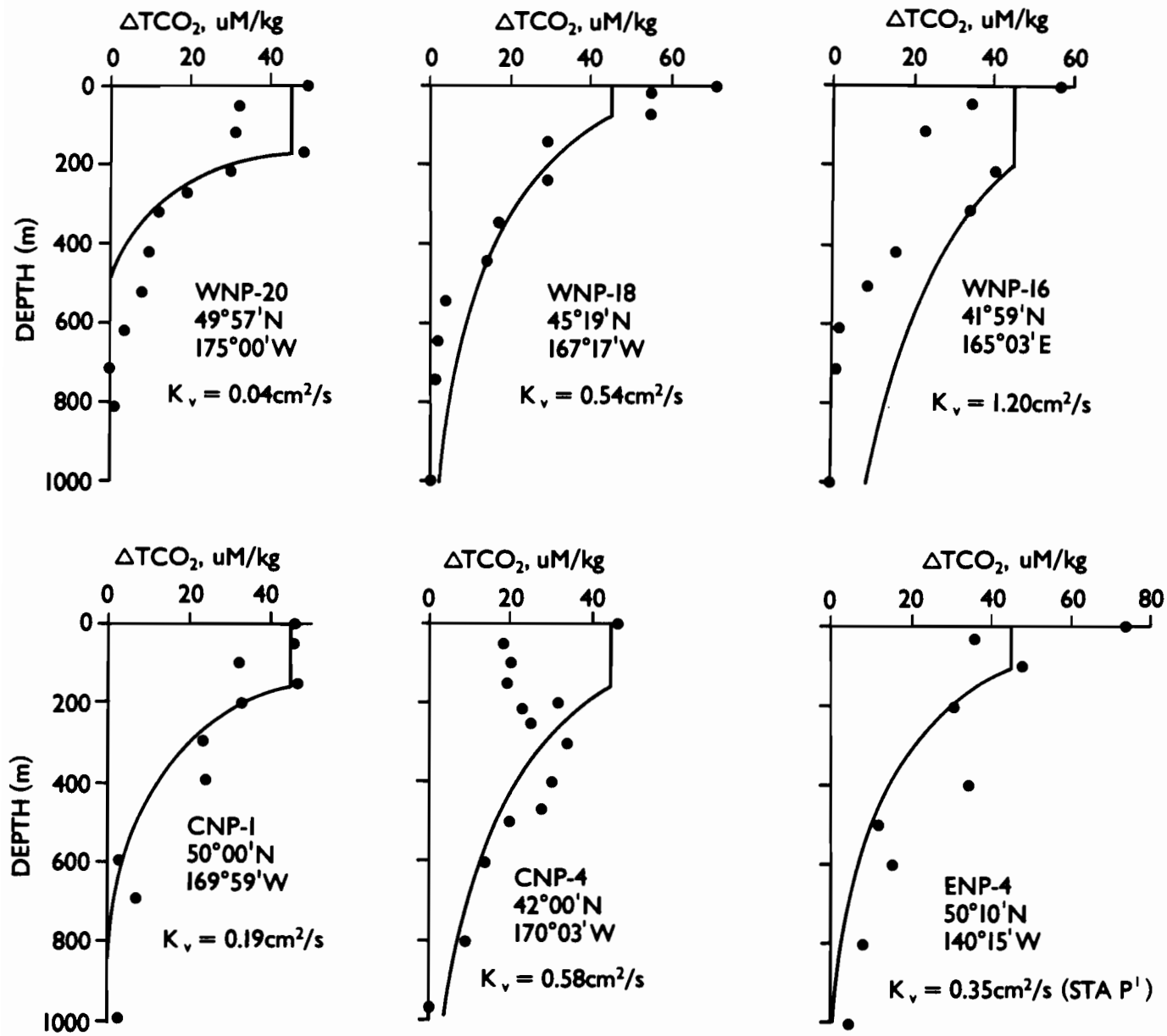

Figure 5.1 Comparison of the predicted excess TCO_2 profiles in the North Pacific gyre based on modeled parameters derived from the freon-11 distribution and CO_2 source function with the calculated values of excess CO_2 using the back-calculation method.

the subarctic boundary (Table 4.1). Station WNP-16 notwithstanding, the model profiles were similar in shape to the observed profiles. By increasing the surface concentration of excess CO_2 or by increasing the TCO_2 mixed layer depth, or both the model fits could be improved at most stations. There also may be a bias in the way in which the ΔTCO_2 was calculated because they are not seasonally averaged, consequently further tinkering with model parameters would be non-productive.

The poorest fit was obtained at WNP-16, where the ΔTCO_2 concentration was observed to decrease more rapidly with depth than predicted by the model. We ascribe this to complex mixing along the northern boundary of the Kuroshio Extention, which precludes either a simple explanation or accurate calculation of the excess CO_2 profiles. Salinity, temperature and freon-11 all suggest deep ventilation along the front in winter, hence the lack of agreement shown in Fig. 5.1 indicates that the back-calculation method may not be accurate in frontal regimes where complex water mass interactions occur.

The excess CO_2 source function and atmospheric pCO_2 curve are shown in Fig. 4.4. A pre-industrial value of 270 ppm was assumed and a smooth curve was arbitrarily drawn that passes through the observations since 1958 (Keeling, 1980). Minor changes in the source function prior to 1958 were tried, but none made any significant changes in the model profiles. Specifically, we imposed arbitrarily a 5 μM/kg TCO_2 change in 1920 to mimic the terrestrial contribution shown by Broecker and Peng (1982) with no significant change in any of the vertical profiles. We conclude that the model profiles are relatively insensitive to minor changes in the pCO_2 source function, and that the function derived by Broecker and Peng (1982) gives an adequate fit to the observations, the preindustrial intercept

notwithstanding. Subtle changes in the pCO_2 source function, such as those depicted by Broecker and Peng (1982), could not be discerned by our procedure unless significant improvements were made in the ΔTCO_2 calculation.

5.2 Model Predictions of Excess CO_2 in the North Pacific Gyre

The curves shown in Fig. 5.1 were integrated from the surface to about 1000 m to calculate the water column inventory of excess CO_2. The area of interest lies between 40°N and 57°N (16.5×10^6 km^2; Levitus, 1982). The mixed layer, assumed here to be the upper 150 m on the average, contained about 1.1×10^{14} moles of excess CO_2, whereas below 150 m the amount was 1.9×10^{14} moles. The total amount of excess CO_2 in the North Pacific subarctic gyre is therefore about 3.0×10^{14} moles or about 18.2 moles/m^2.

How do these estimates compare to the total amount of CO_2 released? Broecker and Peng (1982) give an integrated CO_2 production of 33×10^{15} moles since 1825. If our estimate of the CO_2 uptake in the North Pacific subarctic gyre were representative of the global ocean, which it is not, we would predict an oceanic uptake of 6.7×10^{15} moles, or about 20% of the total. The North Pacific subarctic gyre is only about 4.5% of the total ocean surface. In all likelihood, the above percentage is small because the North Pacific is not characterized by deep convection mixing as is the case in the North Atlantic and the Southern Ocean. Moreover, we have not included the subtropical gyres, which are apt to contain larger amounts of excess CO_2 because lateral mixing brings CO_2 saturated water into the main thermocline.

The effect of downward transport along isopycnal outcrops is clearly shown by the inventories of bomb-derived ^3H and ^{14}C (Broecker and Peng,

1982). Comparing the north temperate ocean with the North Atlantic and Pacific, after adjusting for area, it is seen that about 34% more ^{14}C resides in the subtropical gyres. This percentage would be even larger if the comparison was made for the North Pacific, because there is not deep water mass formation, which tends to increase the North Atlantic inventory of bomb carbon, and by analogy the amount of excess CO_2 as well.

The relatively small amount of excess CO_2 found in the North Pacific is due largely to the small apparent diffusion coefficient derived from the distribution of F-11. The global model used by Broecker and Peng (1982) and others assumed a mean diffusion coefficient of about 1.6 cm^2/s compared to a mean value assumed here of 0.7 cm^2/s. Since the vertical inventory of excess CO_2 is proportional to the $\sqrt{K_v}$ in the 1-D model, our prediction is about 50% less than would have been predicted from the global averaged model. However, fine structure and vertical heat transfer measurements suggest that K_v is indeed small for the North Pacific subarctic gyre (Gargett, 1984) and further indicates the need for regional modeling of excess CO_2 rather than using a global-averaged 1-D model. In this regard, the next step to be taken to improve the estimate of excess CO_2 in the oceans is to increase the precision and accuracy of the excess CO_2 calculation and to test it against the predictions of other tracers (e.g. freons, ^3H, ^{14}C, and ^{85}Kr). The permanent thermocline of the subtropical gyre of the North Pacific should be the region examined.

6.0 CONCLUSIONS

The distributions of freon-11 were combined with precise total carbon dioxide, total alkalinity, oxygen, nutrient and hydrographic measurements to estimate the amount of excess CO_2 in the subarctic waters of the

North Pacific gyre. The approach we employed utilizes the F-11 profiles to determine the apparent vertical eddy diffusivity. These parameters were input into a zonally averaged, one-dimensional vertical diffusion model along with a carbon dioxide source function to provide vertical profiles of anthropogenic CO_2 concentrations. The model predictions were then compared with estimates of excess CO_2 based on the back-calculation method, which relies on precise measurements of TCO_2, alkalinity, O_2, and nutrients.

The results generally show good agreement between the model profiles and the calculated data for all stations north of the subarctic front. In the region of the front, the model assumptions are apparently not applicable due to the complexity of water mass interactions. Our estimate indicates that approximately 3×10^{14} Moles (3.6×10^{15}g C) of excess carbon has been assimilated by the mixed layer and thermocline waters of the North Pacific gyre. Of the total amount released (about 33×10^{15} Moles or 4×10^{17}g C), the North Pacific gyre only harbors about 1% of it, although the study area was 4.5% of the total surface area of the ocean. This is equivalent to about 2% of the fossil-fuel-derived carbon input to the atmosphere. The distributions of the bomb transients (e.g. ^{3}H, ^{14}C) also suggests that the North Pacific subarctic gyre is a relatively small reservoir of excess CO_2 and that the temperate ocean (15° to 40°) will be a more significant reservoir.

7.0 ACKNOWLEDGMENTS

This work was supported by grants from the Air Resources Laboratory of NOAA to the Pacific Marine Environmental Laboratory. We thank L. Machta, director of the Air Resources Laboratory, for his continued interest and support of this component of the NOAA CO_2 Research Program.

REFERENCES

Almgren, T., D. Dyrssen, M. Strandberg, 1977. Computerized high-precision titrations of some major constituents of sea water onboard the R.V. DMITRY MENDELEEV, *Deep-Sea Res.*, *24*: 325-364, 1977.

Bolin, B., 1960. On the exchange of carbon dioxide between the atmosphere and the sea. *Tellus*, *12*: 244-281.

Bos, D. L., and R. T. Williams, 1982. History and development of the GEOSECS alkalinity titration system, H. G. Ostlund and D. Dyrssen (eds.), Proceedings on Workshop on Oceanic CO_2 Standardization, Carbon Dioxide Effects Research and Assessment Program, U.S. Department of Energy, CONF-7911173, pp. 42-59, Washington, D.C.

Bradshaw, A. C., P. G. Brewer, D. K. Shafer, and R. T. Williams, 1981. Measurements of total carbon dioxide and alkalinity by potentiometric titration in the GEOSECS program. *Earth Planet. Sci. Lett.*, *55*: 99-115.

Brewer, P. G., 1978. Direct observations of the oceanic CO_2 increase. *Geophys. Res. Lett.*, *5*: 997-1000.

Broecker, W. S., Y. H. Li, and T.-H. Peng, 1971. Carbon dioxide - man's unseen artifact. In: *Impingement of Man in the Oceans*, D. W. Hood (ed.), Wiley-Interscience, New York, 287-324.

Broecker, W. S. and T. H. Peng, 1974. Gas exchange rates between air and sea. *Tellus*, *26*: 21-35.

Broecker, W. S., T. Takahashi, H. J. Simpson, and T.-H. Peng, 1979. Rate of fossil fuel carbon dioxide and global carbon budget. *Science*, *206*: 409-418.

Broecker, W. S., T. H. Peng, and T. Takahashi, 1980. A strategy for the use of bomb-produced radiocarbon as a tracer for the transport of fossil fuel CO_2 into the deep-sea source regions. *Earth Planet. Sci. Lett.*, *49*: 53-462.

Broecker, W. S. and T. H. Peng, 1982. *Tracers in the Sea*. Lamont-Doherty Geological Observatory, Columbia University, Palisades, New York, 10964, 690 pp.

Chen, C. T. and F. J. Millero, 1979. Gradual increase of oceanic carbon dioxide. *Nature, 277*: 205-206.

Chen, C. T., and R. M. Pytkowicz, 1979. On the total CO_2--titration alkalinity--oxygen system in the Pacific Ocean. *Nature, 281*: 362-365.

Chen, C. T., 1982. Oceanic penetration of excess CO_2 in a cross section between Alaska and Hawaii. *Geophys. Res. Lett., 9*: 117-119.

Chen, C. T., F. J. Millero, and R. M. Pytkowicz, 1982. Comments on "Calculating the oceanic CO_2 increase: A need for caution by A. M. Shiller." *J. Geophys. Res., 87(3)*: 2083-2085.

Cline, J. D., H. B. Milburn, and D. P. Wisegarver, 1982. A simple rosette-mounted syringe sampler for the collection of dissolved gases. *Deep-Sea Res., 29*: 1245-1250.

Cline, J. D., R. H. Gammon, and D. P. Wisegarver, submitted for publication. Distribution of dissolved trichlorofluoromethane (F-11) in the eastern North Pacific with emphasis on vertical transport in the subarctic gyre.

Craig, H., 1957. The national distribution of radiocarbon and the exchange time of carbon dioxide between the atmosphere and sea. *Tellus, 9*: 1-17.

Culkin, F., 1965. The major constituents of sea water. In *Chemical Oceanography*, Vol. 1, J. P. Riley and G. Skirrow, editors, Academic Press, New York, 121-158.

Dodimead, A. J., F. Favorite and T. Hirano, 1962. Review of oceanography of the subarctic Pacific region. *Bull. Internat. N. Pacif. Fish. Comm., 13*: 1-195.

Dodimead, A. J., F. Favorite, and T. Hirano, 1963. Salmon of the north Pacific Ocean, Part II. Review of oceanography of the subarctic Pacific region, *Int. North Pac. Fish. Comm. Bull., 13*: 1-195.

DOE, 1983. *CO_2 Climate Research*, DOE/ER-0186, December 1983, Office of Energy Research, Carbon Dioxide Research Division, Washington, D.C. 20545, 22 pp.

Dyrssen, D., and L. G. Sillen, 1967. Alkalinity and total carbonate in seawater; a plea for P-T-independent data, *Tellus, 19*: 113-121.

Edmond, J. M., 1970. High precision determination of titration alkalinity and total carbon dioxide of seawater by potentiometric titration. *Deep Sea Res., 17*: 737-750.

Gammon, R. H., J. D. Cline and D. P. Wisegarver, 1982. Chlorofluoromethanes in the northeast Pacific Ocean: Measured vertical distributions and applications as transient tracers of upper ocean mixing. *J. Geophys. Res., 87*: 9441-9454.

Gargett, A.E., 1984, Vertical eddy diffusivity in the ocean interior, *J. Mar. Res., 42*, 359-393.

Keeling, C. D., 1973. The carbon dioxide cycle: reservoir models to depict the exchange of atmospheric carbon dioxide with the oceans and land plants. In: *Chemistry of the Lower Atmosphere*, S. I. Rasool (ed.), 251-329.

Keeling, C. D., 1980. The oceans and biosphere as future sinks for fossil fuel carbon dioxide. In: *Interactions of Energy and Climate*, W. Bach, J. Pankrath, and J. Williams (eds.), pp. 129-147, D. Reidel Publishing Company.

Khalil, M. A. K., and R. A. Rasmussen, 1981. Decline in the atmospheric accumulation rates of $CFCl_3$ (F-11), CCl_2F_2 (F-12) and CH_3CCl_3. *J. Air Pollut. Constr. Ass., 31*: 1274-1275.

Levitus, S., 1982. Climatological Atlas of the World Ocean. *NOAA Professional Paper No. 13*, U.S. Government Printing Office, Washington, D.C., 173 pp.

Lyman, J., 1956. Buffer mechanism of seawater. Ph.D Thesis. University of California, Los Angeles, 196 pp.

Manabe, S. and R. T. Wetherald, 1975. The effect of doubling the CO_2 concentration on the climate of a general circulation model. *J. Atmos. Sci., 32*: 3-15.

Manabe, S. and R. T. Wetherald, 1980. On the distribution of climate change resulting from an increase in CO_2 content of the atmosphere. *J. Atmos. Sci., 37*: 99-118.

McCarthy, R. L., F. A. Bower, and J. P. Jesson, 1977. The fluorocarbon-ozone theory, 1, Production and release of CCl_3F and CCl_2F_2 through 1975. *Atmos. Environ., 11*: 491-497.

Mehrbach, C., C. H. Culberson, J. E. Hawley, and R. M. Pytkowicz, 1973. Measurements of the apparent constants of carbonic acid in seawater at atmospheric pressure. *Limnol. Oceanogr., 18*: 897-907.

Millero, F. J., 1979: The thermodynamics of the carbonate system in seawater. *Geochim. Cosmochim. Acta., 43*: 1651-1661.

National Research Council, 1979. *Carbon Dioxide and Climate: A Scientific Assessment*. National Academy Press, Washington, D.C.

National Research Council, 1982. *Carbon Dioxide and Climate: A Second Assessment*. National Academy Press, Washington, D.C.

Oeschger, H., U. Siegenthaler, U. Schotterer, and A. Gugelmann, 1975. A box diffusion model to study the carbon dioxide exchange in nature. *Tellus, 27*: 168-192.

Reid, J. L., 1965. Intermediate waters of the Pacific Ocean. *The Johns Hopkins Oceanogr. Studies, No. 2*, Johns Hopkins Univ. Press, Baltimore, MD, 85 pp.

Reid, J. L., 1969. Sea-surface temperature, salinity, and density of the Pacific Ocean in summer and in winter. *Deep-Sea Res., 16*: 215-224.

Reid, J. L., 1973a. The shallow salinity minima of the Pacific Ocean. *Deep-Sea Res., 20*: 51-68.

Reid, J. L., 1973b. Northwest Pacific Ocean waters in winter. *The Johns Hopkins Oceanographic Studies, No. 5*, Johns Hopkins Univ. Press, Baltimore, MD, 96 pp.

Robinson, M. K. and R. A. Bauer, 1976. Atlas of North Pacific Ocean Monthly Mean Temperatures and Mean Salinities of the Surface Layer. *Ref. Publ. No. 2, Naval Oceanographic Office*, Washington, D.C. 20373.

Roden, G. I., 1980. On the subtropical frontal zone north of Hawaii during winter. *J. Phys. Oceanogr., 10*: 342-362.

Roden, G. I., 1981. Mesoscale thermohaline, sound velocity and baroclinic flow structure of the Pacific subtropical front during the winter of 1980. *J. Phys. Oceanogr., 11*: 658-675.

Shiller, A. M., and J. M. Gieskes, 1980. Processes affecting the oceanic distributions of dissolved calcium and alkalinity. *J. Geophys. Res., 85*: 2719-2727.

Strickland, J. D. H. and T. R. Parsons, 1972. *A Practical Handbook of Seawater Analysis*. Fisheries Research Board of Canada, Ottawa, Canada.

Sverdrup, H. U., M. W. Johnson, and R. H. Fleming, 1942. *The Oceans*. Prentice-Hall, Inc., Englewood Cliffs, N.J., 1087 pp.

Swinnerton, J. W., Linnenbom, V. J., 1967. Determination of the C_1-C_4 hydrocarbons in seawater by gas chromatography. *J. Gas Chromatogr., 5*: 570-573.

Takahashi, T., R. T. Williams and D. L. Bos, 1982. Carbonate chemistry. In: W. S. Broecker, D. W. Spencer, and H. Craig (editors) *GEOSECS Pacific Expedition Volume 3, Hydrographic Data*, pp. 78-82, National Science Foundation, Washington, D.C.

Takahashi, T., D. Chipman, and T. Volk, 1983. Geographical, seasonal and secular variations of the partial pressure of CO_2 in surface waters of the north Atlantic Ocean: the results of the North Atlantic TTO Program. In: *Proceedings Carbon Dioxide Research Conference: Carbon Dioxide, Science and Consensus*. United States Department of Energy, CONF-820970, pp. 123-146.

Wisegarver, D. P. and J. D. Cline, 1984: Solubility of trichlorofluoromethane (F-11) and dichlorodifluoromethane (F-12) in seawater and its relationship to surface concentrations in the North Pacific. *Deep-Sea Res.* (in press).

APPENDIX 1

Chemical and Hydrographic Data for the North Pacific Gyre

WNP20 LAT 49 59.5 N LONG 175 1.0 E DATE: 19 JUNE 82

Depth m	Temp. Deg C	Theta Deg C	Salinity °/oo	Sigma-t	D.O. µM/kg	AOU µM/kg	SIO_4 µM/kg	PO_4 µM/kg	NO_3 µM/kg	Alk meq/kg	TCO_2 mM/kg
1	5.84	5.84	32.678	25.740	316	-9	12.9	0.86	10.4	2.224	2.046
54	5.12	5.12	32.680	25.825	316	-3	13.6	0.88	10.2	2.216	2.037
123	3.64	3.63	33.597	26.708	115	206	69.8	2.32	35.6	2.272	2.252
172	3.62	3.61	33.889	26.942	77	244	94.6	2.73	42.8	2.300	2.319
222	3.59	3.58	33.966	27.007	39	282	101.3	2.76	42.2	2.312	2.337
271	3.55	3.53	34.020	27.053	23	298	108.1	2.80	43.4	2.320	2.344
320	3.51	3.49	34.077	27.103	19	302	112.9	2.81	43.4	2.327	2.346
418	3.42	3.40	34.156	27.174	20	302	112.0	2.78	42.4	2.342	2.356
517	3.21	3.18	34.225	27.249	20	303	120.7	2.60	38.8	2.356	2.366
615	3.08	3.04	34.278	27.303	20	305	133.4	2.78	42.8	2.362	2.370
713	2.94	2.90	34.326	27.354	19	307	139.2	2.73	42.6	2.370	2.374
812	2.81	2.76	34.366	27.398	21	305	147.9	2.72	41.4	2.379	2.382
1015	2.58	2.52	34.423	27.463	25	303	--	2.76	42.8	2.361	2.370
1261	2.31	2.24	34.488	27.538	34	296	143.1	2.78	42.8	2.377	2.383
1512	2.06	1.98	34.542	27.602	53	279	168.4	2.66	41.9	2.409	2.392
2007	1.77	1.66	34.628	27.693	82	253	160.6	2.48	37.1	2.412	2.392
2505	1.64	1.50	34.633	27.707	103	232	171.3	2.45	38.7	2.418	2.385
3002	1.55	1.38	34.656	27.732	126	211	171.3	2.35	37.5	2.421	2.371

Depth m	Temp. Deg C	Salinity °/oo	Sigma-t	F11 pmol/l	F12 pmol/l
3	5.910	32.66	25.717	4.141	1.805
47	5.370	32.67	25.789	4.210	1.834
100	3.620	33.14	26.327	3.261	
151	3.650	33.82	26.884	0.859	0.399
200	3.620	33.94	26.983	0.523	0.377
297	3.560	34.06	27.084	0.215	0.158
348	3.510	34.11	27.129	0.147	0.111
396	3.450	34.13	27.151	0.154	0.077
497	3.320	34.21	27.227	0.094	0.058
598	3.187	34.27	27.287		
698	3.030	34.31	27.333		
786				0.046	--
117	3.720	33.62	26.718	2.095	1.053
143	3.640	33.82	26.885	--	--
243	3.600	34.02	27.049	0.492	0.290
786	2.910	--	--	0.047	0.046
44	5.790	32.68	25.748	4.136	1.812
69	4.490	32.83	26.012	3.910	1.669
95	3.950	33.22	26.377	3.153	1.823
143	3.670	33.81	26.875	1.007	0.497
190	3.620	33.94	26.983	0.436	--

WNP 18 LAT 45 17.4 N LONG 167 15.9 E DATE: 17 JUNE 82

Depth m	Temp. Deg C	Theta Deg C	Salinity °/oo	Sigma-t	D.O. µM/kg	AOU µM/kg	SIO_4 µM/kg	PO_4 µM/kg	NO_3 µM/kg	Alk meq/kg	TCO_2 mM/kg
1	5.62	5.62	32.903	25.944	335	-27	32.5	1.51	17.8	2.226	2.064
73	2.13	2.13	33.108	26.447	336	-1	42.1	1.73	23.9	2.243	2.118
143	2.58	2.57	33.403	26.648	265	65	43.8	1.81	24.5	2.258	2.151
243	3.11	3.10	33.698	26.838	136	190	76.7	2.53	34.7	2.286	2.255
344	3.76	3.74	33.968	26.992	87	233	87.3	2.67	37.3	2.312	2.288
443	3.15	3.13	34.000	27.075	54	271	112.0	2.91	41.5	2.324	2.327
542	3.32	3.23	34.149	27.178	42	281	108.1	2.85	38.7	2.342	2.336
642	3.33	3.29	34.229	27.241	38	285	117.8	2.93	40.4	2.344	2.340
742	3.08	3.04	34.274	27.300	35	290	123.6	2.96	40.8	2.362	2.356
842	2.90	2.85	34.322	27.355	28	298	141.1	2.94	41.9	2.371	2.370
1040	2.69	2.63	34.410	27.444	37	291	147.0	2.87	40.6	2.388	2.378
1291	2.35	2.26	34.476	27.525	40	291	--	2.93	40.6	2.402	2.374
1540	2.15	2.07	34.535	27.569	49	283	157.7	2.91	40.5	2.395	2.374
2040	1.85	1.74	34.613	27.675	78	256	161.5	2.74	38.0	2.411	2.368
2209	1.76	1.64	34.617	27.685	90	245	159.6	2.74	38.8	2.413	2.363
2538	1.62	1.46	34.639	27.713	110	226	--	2.61	--	2.412	2.347
3038	1.51	1.33	34.664	27.741	132	205	164.4	2.53	38.2	2.412	2.338

WNP18 CAST: 125 LAT 45 15.9 N LONG 167 18.1 E DATE: 16 JUNE 82

Depth m	Temp. Deg C	Salinity °/oo	Sigma-t	F11 pmol/l	F12 pmol/l
44	3.85	33.03	26.236	4.237	1.770
95	2.45	33.19	26.488	4.350	1.878
193	2.84	33.58	26.767	2.448	1.026
440	3.41	34.03	27.075	0.585	0.267
493	3.30	34.08	27.125	0.256	0.126
590	3.36	34.21	27.223	0.256	0.126
99	1.82	33.13	26.488	4.558	1.984
199	2.75	33.61	26.799	2.318	0.958
298	3.42	33.85	26.930	1.353	0.583
400	3.19	33.96	27.040	0.781	0.371
498	3.44	34.12	27.144	0.351	0.196
598	3.37	34.21	27.222	0.236	0.136
699	3.19	34.28	27.295	0.162	0.064
798	2.99	34.32	27.345	0.114	0.062
1000	2.72	34.41	27.441	0.103	0.032
4	5.66	32.91	25.945	4.257	1.856
46	3.80	33.06	26.265	4.030	2.106
144	3.16	33.49	26.667	3.199	1.408
216	3.28	33.73	26.848	1.829	0.814
242	3.12	33.76	26.886	1.747	0.742
268	3.96	33.79	26.830	1.435	0.622
294	3.54	33.92	26.975	1.093	0.499
318	3.53	33.95	27.000	0.894	0.399
339	3.25	33.96	27.034	0.880	0.384
391	3.13	34.00	27.077	0.699	0.344

WNP 16 LAT 41 58.1 N LONG 165 2.6 E DATE: 15 JUNE 82

Depth m	Temp. Deg C	Theta Deg C	Salinity °/oo	Sigma-t	D.O. µM/kg	AOU µM/kg	SIO_4 µM/kg	PO_4 µM/kg	NO_3 µM/kg	Alk meq/kg	TCO_2 mM/kg
1	9.92	9.92	33.415	25.730	296	-18	17.2	0.85	9.3	2.242	2.033
45	7.29	7.29	33.647	26.316	297	-2	16.6	0.94	10.6	2.243	2.058
114	5.61	5.60	33.824	26.674	284	22	25.5	1.17	16.4	2.258	2.094
214	6.10	6.08	33.904	26.677	212	90	42.5	1.66	23.5	2.283	2.169
316	4.34	4.32	33.897	26.876	161	155	69.3	2.30	32.3	2.292	2.232
412	4.32	4.29	34.040	26.991	94	221	78.4	2.29	29.0	2.305	2.272
512	3.74	3.71	34.138	27.129	57	263	98.3	2.51	33.4	2.329	2.316
612	3.81	3.77	34.249	27.210	50	268	112.9	2.81	39.9	2.336	2.320
710	3.45	3.41	34.303	27.289	46	275	122.7	2.88	40.8	2.354	2.339
810	3.25	3.20	34.376	27.366	40	282	130.4	2.92	40.6	2.360	2.345
1005	2.82	2.76	34.419	27.439	36	290	136.3	2.93	40.5	2.384	2.374
1256	2.46	2.39	34.492	27.529	39	290	146.0	3.00	40.6	2.396	2.381
1505	2.19	2.11	34.545	27.594	50	282	135.3	2.97	39.9	2.405	2.379
1997	1.87	1.76	34.623	27.681	79	255	148.9	2.82	38.2	2.416	2.376
2498	1.62	1.48	34.664	27.733	111	225	145.0	2.64	36.6	2.423	2.359
2998	1.53	1.36	34.687	27.758	130	206	131.4	2.55	34.1	2.419	2.341

WNP 16 CAST: 107 LAT 41 58.8 N LONG 165 03.1 E 14 JUNE 82

Depth m	Temp. Deg C	Salinity °/oo	Sigma-t	F11 pmol/l	F12 pmol/l
3	10.88	33.50	25.631	3.143	1.461
43	9.58	33.75	26.048	3.369	1.638
94	7.17	33.85	26.492	3.254	1.690
145	6.56	33.80	26.535	3.171	1.348
193	6.40	33.87	26.611	2.901	1.214
243	5.52	33.91	26.753	2.333	0.942
292	4.13	33.75	26.781	2.228	0.887
341	4.58	33.92	26.868	1.285	0.521
391	4.14	33.95	26.939	0.941	0.430
439	4.16	34.04	27.008	0.578	0.316
489	3.88	34.07	27.061	0.487	0.225
583	3.92	34.19	27.152	0.252	0.101
750	3.56	34.27	27.252	0.062	0.048
901	2.32	34.40	27.467	0.033	0.046
1097	2.90	34.40	27.417	0.040	0.017
1198	2.57	34.46	27.494		

CNP 1 LAT 50 1.5 N LONG 170 1.4 W DATE: 4 March 83

Depth m	Temp. Deg C	Theta Deg C	Salinity °/oo	Sigma-t	D.O. µM/kg	AOU µM/kg	SIO_4 µM/kg	PO_4 µM/kg	NO_3 µM/kg	Alk meq/kg	TCO_2 mM/kg
1	2.840	2.84	32.837	26.174			24.6	1.29	15.4	2.202	2.081
9	2.830	2.83	32.750	26.328	320	11	25.9	1.28	14.7	2.214	2.084
49	2.820	2.82	32.674	26.045	320	10	15.5	1.02	6.8	2.211	2.081
98	2.880	2.87	32.844	26.176	280	30	27.4	1.37	15.2	2.213	2.087
148	3.230	3.22	33.660	26.797	140	184	71.8	2.46	36.2	2.281	2.263
197	3.270	3.26	33.809	26.912	80	244	89.0	2.73	40.7	2.294	2.302
296	3.510	3.49	34.004	27.045	30	292	108.5	2.93	45.1	2.310	2.339
395	3.480	3.45	34.102	27.126	35	286	115.4	2.93	44.1	2.320	2.345
593	3.170	3.13	34.245	27.269	24	300	137.0	2.91	44.3	2.364	2.364
692	3.030	2.98	34.295	27.321	26	299	140.9	2.86	44.1	2.366	2.372
791	2.880	2.83	34.343	27.373	--	--	145.9	--	44.3	2.369	2.377
989	2.690	2.63	34.404	27.439	27	300	160.0	2.88	44.3	2.380	2.383
1483	2.170	2.07	34.522	27.577	45	286	179.4	2.90	44.1	2.391	2.392
1978	1.870	1.74	34.606	27.668	71	263	181.1	2.72	42.3	2.411	2.383
2472	1.670	1.50	34.633	27.704	98	238	181.1	2.61	40.5	2.418	2.379
2967	1.580	1.36	34.658	27.731	--	--	173.1	2.48	39.2	2.414	2.359
3610	1.465	1.19	34.676	27.754	144	193	167.4	2.45	37.9	2.411	2.341
3857	1.465	1.16	34.682	27.759	183	154	170.1	2.32	37.3	2.421	2.340

CNP 1 CAST: 2 LAT 50 00.1 N LONG 169 59.4 W DATE: 5 MAR 83

Depth m	Temp. Deg C	Salinity °/oo	Sigma-t	F11 pmol/l
8	2.821	32.769	26.121	4.67
23	2.821	32.760	26.114	4.57
50	2.821	32.767	26.120	4.65
103	3.215	33.943	27.024	4.27
126	3.233	33.453	26.631	2.98
149	3.162	33.599	26.754	2.22
179	3.162	33.687	26.824	2.05
202	3.197	33.742	26.865	1.66
229	3.215	33.792	26.903	1.79
252	3.305	33.832	26.944	1.18
305	3.466	33.946	27.003	0.85
351	3.502	33.988	27.033	0.84
397	3.448	34.102	27.129	0.52
499	3.340	34.182	27.203	0.46
598	3.197	34.259	27.277	0.13
800	2.893	34.349	27.377	0.00

CNP 2 CAST: 7 LAT 46 59.8 N LONG 169 59.2 W DATE: 6 March 83

Depth m	Temp. Deg C	Salinity °/oo	Sigma-t	F11 pmol/l
8	3.894	32.983	26.194	4.52
23	3.895	32.975	26.188	4.82
50	3.895	32.981	26.193	4.65
103	3.895	32.994	26.203	--
121	3.913	32.967	26.180	4.43
152	3.967	33.468	26.573	3.44
179	3.895	33.629	26.708	2.73
195	3.859	33.679	26.752	2.22
225	3.877	33.738	26.797	1.82
252	3.895	33.775	26.824	1.52
305	3.806	33.821	26.870	1.10
351	3.788	33.896	26.931	--
397	3.770	33.952	26.978	0.60
503	3.609	34.064	27.083	0.57
598	3.466	34.143	27.160	0.34

CNP 3 LAT 45 1.0 N LONG 170 1.0 W DATE: 7 MARCH 83

Depth m	Temp. Deg C	Theta Deg C	Salinity °/oo	Sigma-t	D.O. µM/kg	AOU µM/kg	SIO_4 µM/kg	PO_4 µM/kg	NO_3 µM/kg	Alk meq/kg	TCO_2 mM/kg
1	3.97	3.97	33.180	26.344			21.1	1.26	12.9	2.232	2.069
9	4.08	4.08	33.098	26.610	310	9	20.8	1.13	12.7	2.228	2.068
49	4.41	4.41	33.103	26.238	314	3	15.4	0.99	7.5	2.228	2.062
98	4.40	4.39	33.127	26.258	314	3	21.2	1.17	12.7	2.229	2.063
148	5.53	5.52	33.495	26.423	284	24	26.0	1.25	14.4	2.231	2.091
198	5.19	5.18	33.753	26.667	244	66	37.3	1.50	20.1	2.264	2.138
247	4.78	4.76	33.783	26.738	203	109	38.4	1.56	17.8	2.276	2.177
297	4.64	4.61	33.822	26.784	161	152	60.5	2.00	29.4	2.274	2.214
396	4.13	4.10	33.933	26.927	100	217	81.0	2.38	33.6	2.305	2.272
495	3.94	3.91	34.016	27.012	86	233	93.4	2.60	38.8	2.316	2.304
991	2.90	2.83	34.210	27.265	68	258	131.2	2.70	40.1	2.367	2.334
1238	2.60	2.52	34.437	27.472	31	297	160.5	2.82	41.6	2.390	2.393
1486	2.35	2.25	34.503	27.547	33	297	173.6	2.85	44.2	2.402	2.397
1982	1.93	1.80	34.588	27.649	60	273	185.2	2.78	42.6	--	2.375
2477	1.70	1.53	34.625	27.696	67	268	183.3	2.59	40.7	2.414	2.371
3468	1.49	1.23	34.669	27.747	136	201	172.0	2.29	33.5	2.411	2.340
3964	1.47	1.16	34.664	27.744	148	189	166.5	2.21	31.2	2.423	2.340

CNP 4 LAT 41 59.4 N LONG 170 1.5 W DATE: 8 MARCH 83

Depth m	Temp. Deg C	Theta Deg C	Salinity °/oo	Sigma-t	D.O. µM/kg	AOU µM/kg	SIO_4 µM/kg	PO_4 µM/kg	NO_3 µM/kg	Alk meq/kg	TCO_2 mM/kg
1	8.29	8.29	33.884	26.357	278	9	7.2	0.58	3.6	2.211	2.058
10	8.07	8.07	33.869	26.378	278	11	13.7	0.78	8.1	2.266	2.058
50	8.04	8.03	33.868	26.381	280	9	14.3	0.83	8.5	2.255	2.054
100	8.08	8.07	33.868	26.375	280	9	14.4	0.81	8.6	2.256	2.056
150	8.09	8.07	33.869	26.375	281	8	12.3	0.74	7.0	2.264	2.057
200	8.12	8.10	33.876	26.376	280	9	14.3	0.81	8.5	2.247	2.063
216	8.14	8.12	34.032	26.495	213	75	27.9	1.36	17.5	2.265	2.114
250	7.89	7.86	34.030	26.531	226	64	27.5	1.34	17.7	2.275	2.116
300	6.94	6.91	33.957	26.608	215	81	24.7	0.98	11.7	2.269	2.142
400	5.99	5.96	33.941	26.720	159	144	51.3	2.05	25.5	2.278	2.197
466	5.10	5.06	33.971	26.850	129	180	67.7	2.47	33.3	2.302	2.243
500	4.76	4.72	33.979	26.895	144	168	65.1	2.41	31.5	2.286	2.222
600	4.29	4.24	34.090	27.034	74	241	91.7	2.82	35.6	2.315	2.291
800	3.65	3.59	34.234	27.214	43	277	109.6	2.80	--	2.358	2.345
966	3.23	3.16	34.316	27.320	32	291	128.3	--	43.9	2.363	2.357
1000	3.18	3.11	34.335	27.340	35	288	127.8	--	38.5	2.367	2.370
1466	2.44	2.34	34.486	27.526	25	305	153.2	--	37.5	2.406	2.399
1966	1.97	1.84	34.581	27.640	50	283	--	--	--	2.410	2.386
1991	1.96	1.83	34.582	27.641	52	281	--	--	--	2.417	2.388
3033	1.53	1.31	34.646	27.725	120	217	166.7	--	42.2	2.419	2.357

CNP 4 CAST: 16 LAT 41 59.5 N LONG 170 02.8 W DATE: 9 MAR 83

Depth m	Temp. Deg C	Salinity °/oo	Sigma-t	F11 pmol/l
7	8.092	33.842	26.353	3.11
25	8.092	33.842	26.353	
50	8.092	33.844	26.355	3.46
102	8.102	33.844	26.353	3.56
126	8.092	33.845	26.356	3.24
150	8.102	33.846	26.355	3.41
173	8.112	33.852	26.358	3.52
200	8.157	33.869	26.365	3.33
225	8.342	33.990	26.432	2.87
250	8.112	34.029	26.497	2.56
300	7.172	33.949	26.570	2.93
350	6.302	33.899	26.647	2.63
398	5.719	33.922	26.738	1.47
498	4.737	34.001	26.918	0.70
608	4.326	34.068	27.013	
798	3.693	34.246	27.220	0.11

ENP 2 LAT 54 19.6 N LONG 151 15.4 W DATE: 15 JUNE 81

Depth m	Temp. Deg C	Theta Deg C	Salinity °/oo	Sigma-t	D.O. µM/kg	AOU µM/kg	SIO_4 µM/kg	PO_4 µM/kg	NO_3 µM/kg	Alk meq/kg	TCO_2 mM/kg
1	9.80	9.800	32.330	24.903	276	-10				2.198	1.970
32	7.42	7.410	32.335	25.267	291	5	6.7	0.57	2.1	2.209	1.981
105	5.55	5.540	32.960	25.999	228	80	31.0	1.26	14.8	2.222	2.118
203	4.99	4.980	33.802	26.730	104	207	52.9	1.80	24.4	2.281	2.248
401	3.88	3.860	34.012	27.017	35	284	79.9	2.19	29.5	2.333	2.339
518	3.66	3.620	34.116	27.123	31	290	123.0	2.91	39.7	2.346	2.351
601	3.57	3.530	34.176	27.180	27	294	132.0	2.76	40.5	2.360	2.366
800	3.20	3.150	34.285	27.303	23	301	148.0	2.88	40.5	2.382	2.383
1003	2.87	2.810	34.358	27.392	23	304	154.0	2.94	40.7	2.391	2.390
1251	2.55	2.460	34.441	27.488	26	304	164.0	3.02	41.0	2.414	2.406
1499	2.27	2.170	34.507	27.565	40	292	--	2.99	39.9	2.422	2.403
2003	1.92	1.790	34.581	27.654	65	270	186.0	2.80	39.1	2.438	2.400
2540	1.69	1.510	34.606	27.694	95	242	175.0	2.71	37.4	2.438	2.376

ENP 4 LAT 50 2.3 N LONG 149 59.2 W DATE: 16 JUNE 81

Depth m	Temp. Deg C	Theta Deg C	Salinity °/oo	Sigma-t	D.O. µM/kg	AOU µM/kg	SIO_4 µM/kg	PO_4 µM/kg	NO_3 µM/kg	Alk meq/kg	TCO_2 mM/kg
1	8.70	8.70	32.500	25.209	305	-17				2.200	2.016
32	8.24	8.24	32.499	25.296	305	-14	22.6	1.10	11.8	2.129	1.953
105	4.86	4.86	32.893	26.032	275	38	33.1	1.54	19.8	2.222	2.092
202	3.94	3.93	33.759	26.798	130	189	60.2	1.99	27.0	2.286	2.249
399	3.82	3.79	34.012	27.004	60	259	103.0	2.74	36.9	2.326	2.332
507	3.71	3.68	34.130	27.104	47	274	116.0	2.58	37.1	2.337	2.331
603	3.52	3.48	34.196	27.172	36	285	121.0	2.58	36.2	2.359	2.358
799	3.18	3.13	34.295	27.277	29	295	145.0	2.88	39.9	2.376	2.374
1002	2.85	2.79	34.362	27.356	23	303	159.0	2.98	40.3	2.394	2.391
1251	2.55	2.47	34.446	27.438	26	304	149.0	2.93	39.9	2.411	2.407
1499	2.30	2.21	34.502	27.491	36	295	164.0	2.64	38.0	2.423	2.412
2002	1.97	1.84	34.590	27.568	60	275	182.0	2.77	38.9	2.437	2.406
2658	1.69	1.50	34.662	27.598	93	244	154.0	2.54	37.5	2.440	2.384

ENP 6 LAT 46 0.5 N LONG 150 0.8 W DATE: 19 JUNE 81

Depth m	Temp. Deg C	Theta Deg C	Salinity °/oo	Sigma-t	D.O. µM/kg	AOU µM/kg	SIO_4 µM/kg	PO_4 µM/kg	NO_3 µM/kg	Alk meq/kg	TCO_2 mM/kg
1	8.70	8.70	32.800	25.444	299	-11	0.1	0.01	0.1	2.206	2.009
10	8.60	8.60	32.800	25.460	299	-11	0.1	0.01	0.1	2.186	2.004
29	8.81	8.80	32.787	25.419	299	-12	0.1	--	--	2.212	2.022
50	8.60	8.60	32.740	25.413	298	-10	0.1	0.01	0.1	2.195	2.011
63	8.00	8.00	32.760	25.517	297	-5	0.1	0.01	0.1	2.191	2.006
98	6.87	6.86	32.966	25.838	296	4	21.4	1.00	11.8	2.216	2.039
201	6.39	6.37	33.347	26.202	213	88	40.3	1.49	21.0	2.270	2.147
400	4.53	4.53	33.952	26.899	101	213	85.9	2.37	33.7	2.314	2.279
501	4.16	4.13	34.042	27.013	70	247	102.9	2.52	35.7	2.319	2.302
595	3.95	3.91	34.108	27.088	55	264	120.0	2.66	37.7	2.345	2.332
801	3.42	3.29	34.250	27.262	32	292	134.0	2.78	38.1	2.368	2.364
1007	3.02	2.96	34.345	27.368	20	306	158.0	2.87	40.2	2.390	2.390
1253	2.64	2.56	34.433	27.473	19	310	170.0	2.84	40.8	2.407	2.407
1498	2.35	2.25	34.496	27.549	20	312	182.0	2.77	40.8	2.422	2.411
2003	1.96	1.83	34.574	27.645	55	280	177.0	2.63	36.9	2.440	2.411
2657	1.68	1.50	34.628	27.713	95	243	185.0	2.51	37.7	2.438	2.383

ENP 8 LAT 41 55.7 N LONG 150 8.7 W DATE: 21 JUNE 81

Depth m	Temp. Deg C	Theta Deg C	Salinity °/oo	Sigma-t	D.O. µM/kg	AOU µM/kg	SIO_4 µM/kg	PO_4 µM/kg	NO_3 µM/kg	Alk meq/kg	TCO_2 mM/kg
1	11.00	11.00	32.990	25.213	291	-18	0.1	0.01	0.1	2.225	2.007
30	10.99	10.99	32.924	25.163	291	-18	10.9	0.61	4.6	2.211	1.991
105	8.18	8.08	33.717	26.257	281	8	16.7	0.83	9.2	2.225	2.030
200	8.30	8.28	33.991	26.442	229	58	29.9	1.19	17.2	2.275	2.113
404	5.95	5.91	33.924	26.716	144	160	68.2	2.06	29.8	2.294	2.211
499	4.83	4.79	33.948	26.867	99	213	90.3	2.42	34.8	2.317	2.271
600	4.28	4.24	34.029	26.991	63	252	111.0	2.67	37.5	2.333	2.311
797	3.61	3.56	34.175	27.176	27	294	140.0	2.84	40.9	2.357	2.357
1000	3.10	3.06	34.365	27.375	17	308	156.0	2.93	40.0	2.390	2.393
1251	2.71	2.63	34.383	27.427	16	312	175.0	2.98	41.8	2.408	2.409
1497	2.39	2.29	34.546	27.586	27	304	187.0	2.85	40.8	2.417	2.412
1998	1.96	1.83	34.546	27.623	56	278	197.0	2.73	39.6	2.437	2.406
2653	1.64	1.48	34.614	27.703	93	244	200.0	2.56	38.2	2.443	2.386

STR P′ CAST: 41 LAT 50 14.5 N LONG 140 15.0 W DATE: 2 DEC 80

Depth m	Temp. Deg C	Salinity °/oo	Sigma-t	F11 pmol/l	F12 pmol/l
19	8.20	32.49	25.276	2.76	1.25
41	8.20	32.48	25.269	2.87	1.41
82	8.20	32.48	25.269	3.25	
99	5.89	32.68	25.736	3.49	1.35
149	5.28	33.61	26.544	2.16	0.92
198	5.05	33.79	26.713	1.16	0.44
301	4.33	33.84	26.831	0.69	0.26
396	4.12	33.91	26.909	0.40	0.13
601	3.69	34.04	27.056	0.06	
798	3.29	34.11	27.150	0.08	
1004	2.94	34.15	27.214	0.04	
20	8.04	32.50	25.308	3.06	1.30
40	8.04	32.49	25.300	2.72	1.21
80	8.04	32.48	25.292	2.92	1.28
100	5.87	32.80	25.833	2.77	1.26
125	5.45	33.24	26.231	2.28	1.01
173	5.16	33.75	26.668	1.26	0.53
227	4.75	33.81	26.762	0.86	0.42
299	4.35	33.84	26.829	0.52	0.25
401	4.10	33.92	26.919	0.26	0.16
600	3.67	34.04	27.058	0.08	0.02
804	3.26	34.12	27.161	0.05	0.02
19	7.99	32.49	25.307	3.46	1.32
40	7.99	32.49	25.307	3.59	1.32
77	7.99	32.48	25.299	3.11	1.45
99	5.79	32.75	25.803	3.64	1.47
125	5.38	33.40	26.366	2.32	1.12
176	5.15	33.76	26.677	1.42	0.65
223	4.85	33.82	26.759	0.83	0.45
302	4.37	33.83	26.819	0.59	0.32
399	4.15	33.90	26.898	0.29	0.16
595	3.71	34.03	27.046	0.10	0.07
796	3.29	34.11	27.150	0.06	0.06
19	7.99	32.49	25.307	3.46	1.32
40	7.99	32.49	25.307	3.59	1.32
77	7.99	32.48	25.299	3.11	1.45
99	5.79	32.75	25.803	3.64	1.47
125	5.38	33.40	26.366	2.32	1.12
176	5.15	33.76	26.677	1.42	0.65
223	4.85	33.82	26.759	0.83	0.45
302	4.37	33.83	26.819	0.59	0.32
399	4.15	33.90	26.898	0.29	0.16
595	3.71	34.03	27.046	0.10	0.07
796	3.29	34.11	27.150	0.06	0.06

Depth m	Temp. Deg C	Salinity °/oo	Sigma-t	F11 pmol/l	F12 pmol/
20	7.97	32.49	25.310	3.47	1.36
63	7.98	32.48	25.301	3.39	1.40
99	6.29	32.63	25.647	3.68	1.32
125	5.49	33.23	26.218	2.84	1.10
152	5.29	33.58	26.519	2.12	0.90
174	5.24	33.69	26.612	1.82	0.75
228	4.96	33.80	26.731	1.26	0.62
299	4.40	33.82	26.808	0.85	0.37
401	4.12	33.91	26.909	0.37	0.22
614	3.69	34.05	27.064	0.14	0.05
811	3.25	34.12	27.162	0.16	
20	7.95	32.49	25.313	3.27	1.54
50	7.95	32.48	25.305	3.35	1.61
101	6.25	32.70	25.707	3.49	1.75
111	5.76	32.82	25.862	3.37	1.58
126	5.67	33.02	26.031	3.05	1.57
154	5.31	33.47	26.429	2.30	1.05
203	5.13	33.75	26.672	1.45	0.78
304	4.43	33.83	26.813	0.66	0.37
403	4.12	33.91	26.909	0.29	0.20
607	3.67	34.04	27.058	0.14	0.07
809	3.29	34.12	27.158	0.05	